THERAPEUTIC ADVANCES in
Medical Oncology

Original Research

The antibody–drug conjugate targeting ROR1, NBE-002, is active in high-grade serous ovarian cancer preclinical models

Ther Adv Med Oncol

2025, Vol. 17: 1–20

DOI: 10.1177/17588359251332471

Dongli Liu*, Cassandra J. Vandenberg*, Patrizia Sini, Lorenz Waldmeier, Rosa Baumgartinger, Laura Pisarsky, Georg Petroczi, Gayanie Ratnayake, Clare L. Scott and Caroline E. Ford

Abstract

Background: Novel therapeutics are urgently needed for high-grade serous ovarian cancer (HGSOC). We identified the receptor tyrosine kinase-like orphan receptor 1 (ROR1) as a therapeutic target. NBE-002, an antibody–drug conjugate (ADC) consisting of a humanised anti-ROR1 antibody, huXBR1-402, linked to a highly potent anthracycline-derivative (PNU), has activity in ROR1-positive haematologic malignancies.

Objectives: This study explored the anti-cancer effects of NBE-002 alone and in combination with standard HGSOC therapies, carboplatin, paclitaxel and olaparib.

Design: A ROR1-ADC was tested in cell lines and *in vivo* models of HGSOC.

Methods: Different ROR1-targeting antibodies and payload compositions were constructed and tested *in vitro*. The dose effect of NBE-002 alone and in combination with carboplatin, paclitaxel or olaparib was analysed in ROR1+ HGSOC cell lines. Growth inhibition and apoptosis were monitored by live cell imaging and combination effects determined. Ten HGSOC PDX models were treated with NBE-002 alone, or in combination with carboplatin or olaparib, over 4 weeks and tumour volume and overall survival evaluated.

Results: Synergistic interaction was observed in two out of five HGSOC cell lines treated with NBE-002 and carboplatin (PEO4 and OC023, chemo-resistant), in one out of five treated with NBE-002 and olaparib (PEO1, BRCA2 mutated, HR deficient) and none of five treated with NBE-002 and paclitaxel. In vivo, NBE-002 exhibited activity in PA-1 xenografts and three HGSOC PDX models with high ROR1 expression, platinum sensitivity and homologous recombination DNA repair deficient (HRD). When NBE-002 was combined with carboplatin, activity was observed in 7 of 10 ROR1-expressing PDX models, regardless of platinum or HRD status. The activity was demonstrated in combination with olaparib in both PDX tested, one HRD and one HRD reverted.

Conclusion: The ROR1-targeting ADC, NBE-002, has therapeutic potential in HGSOC, with single agent activity observed both *in vitro* and *in vivo*. Broader clinical applications were evident when NBE-002 was combined with carboplatin or olaparib.

Keywords: antibody–drug conjugates, chemotherapy, chemotherapy resistance, drug screening, ovarian cancer, PARP inhibitors, targeted therapy, translational research

Received: 1 December 2024; revised manuscript accepted: 18 March 2025.

Correspondence to:
Caroline E. Ford
Gynaecological Cancer Research Group, Lowy Cancer Research Centre and School of Clinical Medicine, Faculty of Medicine and Health, Level 2 Lowy Cancer Research Centre, University of New South Wales, Kensington, NSW 2052, Australia
caroline.ford@unsw.edu.au

Dongli Liu
School of Clinical Medicine, Faculty of Medicine and Health, University of New South Wales, Sydney, NSW, Australia

Cassandra J. Vandenberg
The Walter and Eliza Hall Institute of Medical Research, Parkville, VIC, Australia

Department of Medical Biology, University of Melbourne, Melbourne, VIC, Australia

Patrizia Sini
Rosa Baumgartinger
Laura Pisarsky
Georg Petroczi
Boehringer Ingelheim RCV GmbH & Co KG, Wien, Austria

Lorenz Waldmeier
NBE Therapeutics AG, Basel, Switzerland

Gayanie Ratnayake
Royal Women's Hospital, Parkville, VIC, Australia

Clare L. Scott
The Walter and Eliza Hall Institute of Medical Research, Parkville, VIC, Australia

Department of Medical Biology, University of Melbourne, Melbourne, VIC, Australia

Royal Women's Hospital, Parkville, VIC, Australia

Peter MacCallum Cancer Centre, Melbourne, VIC, Australia

*Joint first authors.

Introduction

New approaches to the treatment of high-grade serous ovarian cancer (HGSOC) are needed. Although the introduction of poly-(ADP-ribose) polymerase (PARP) inhibitors (PARPi) for individuals carrying *BRCA1/2* mutations has improved survival for a subgroup of those with HGSOC, overall survival (OS) rates remain poor (5-year survival rate ~50%[1]). The primary treatment approach involves initial cytoreductive surgery and platinum–taxane doublet chemotherapy. For individuals with *BRCA1/2*-mutated or homologous recombination DNA repair deficient (HRD) HGSOC, maintenance therapy with PARPi follows, considered to be standard of care (SoC). Despite generally positive responses to platinum-based chemotherapy, 75% of advanced HGSOC patients will encounter disease recurrence that is ultimately fatal.[2] Up to half of HGSOCs harbour changes in DNA response genes or pathway signatures which are predicted to result in HRD.[3] The approval of PARPi for HRD HGSOC which is in response to platinum-based first-line chemotherapy has significantly enhanced the outlook for those individuals. Conversely, those with an HR proficient (HRP) signature (constituting approximately 50% of women with HGSOC[4]) experience reduced benefits from conventional maintenance therapies involving chemotherapy and the vascular endothelial growth factor (VEGF) inhibitor, antiangiogenic agent, bevacizumab or PARPi.[5] For advanced or recurrent ovarian cancer (OC) patients, bevacizumab was approved, usually in combination with chemotherapy, then as a maintenance treatment, based on clinical evidence.[6–12] While clinical trials exploring alternative targeted therapies have been conducted, these approaches have faced challenges. Immune checkpoint inhibitor (ICI) therapy, alone or in combination with chemotherapy, with or without VEGF inhibition, failed to improve the progression-free survival (PFS) or OS in platinum-resistant or platinum-refractory OC patients, and more recently, even in the first line as combination treatment followed by maintenance therapy.[13,14] However, the post hoc analysis showed that a subgroup of patients with PD-L1 and CD8 tumour expression could benefit from such combined therapies.[13] It is also important to note that in newly diagnosed non-*BRCA*-mutated OC, maintenance therapy with ICIs combined with PARP inhibitors (PARPi) and bevacizumab significantly improved PFS compared to bevacizumab alone, although the specific contribution of ICI to the efficacy of PARPi remains inconclusive.[15]

The receptor tyrosine kinase-like orphan receptor 1 (ROR1) represents a promising biomarker in HGSOC. Comprising both extracellular and intracellular components, ROR1 primarily functions to transmit signals within the non-canonical (β-catenin independent) Wnt signalling pathway.[16] While ROR1 signalling regulates cell polarity, motility and skeletal arrangement in embryonic development, it becomes less essential, with diminished expression observed in the majority of normal tissues throughout adulthood.[17] Intriguingly, ROR1 displays abnormal overexpression in various malignancies including HGSOC, where such elevated expression has been correlated with poor prognosis.[18–20] In our previous study involving 178 OC patients, we observed a significant upregulation of ROR1 in cancer cells compared with the adjacent stroma.[21]

ROR1 signalling and its downstream effector pathways have been extensively investigated in the context of malignancy. Upon binding with its ligand, Wnt5a, ROR1 initiates a series of downstream pathway signals, such as via the Rho family of GTPase activators, and the PI3K/AKT and Hippo-YAP/TAZ pathways, influencing biological processes contributing to tumour proliferation, progression and chemoresistance.[22–24] In HGSOC, inhibiting ROR1 significantly reduced migration and the invasion potential of OC cells *in vitro*.[25,26]

A number of ROR1-targeted therapies have been examined in preclinical studies and clinical trials, and they are of interest due to their unique expression pattern on tumour cells. A humanised ROR1 monoclonal antibody (mAb), zilovertamab (also known as cirmtuzumab or UC-961), has demonstrated safety and efficacy in several phase I/II clinical trials in ROR1-associated malignancies, including chronic lymphocytic leukaemia (CLL), mantle cell lymphoma (MCL) and HER2-negative breast cancer.[27–29] We previously reported that zilovertamab had an anti-proliferative effect in HGSOC *in vitro*.[30] Another chimeric anti-ROR1 Fab antibody (named ROR1-cFab) induced apoptosis, exclusively in ROR1-positive malignancies, both in vitro and in vivo, while exhibiting no effect on ROR1-negative cancers.[31,32]

Efforts have been made recently to develop antibody–drug conjugates (ADCs) targeted to

ROR1-expressing cancers. ADCs consist of a mAb conjugated via a specialised linker to a cytotoxic payload. It is critical that the mAb target antigen is expressed specifically on the surface of cancer cells and not normal tissues, to ensure tolerability and optimal delivery of the ADC to the tumour. Engagement with the target antigen is followed by internalisation, facilitating the release of cytotoxic components intracellularly, ultimately causing cancer cell death. It has been demonstrated that bystander or abscopal effects also contribute to the activity of ADCs,[33] hence cleavage of the linker needs to be restricted to the cancer environment to reduce on-target and off-target toxicity whilst supporting a higher drug-to-antibody-ratio (DAR), which would be associated with higher efficacy – both competitive areas of ADC development. Currently, only one ADC has been approved for the treatment of HGSOC: the folate receptor alpha (FRA)-targeting drug, mirvetuximab soravtansine, a humanised FRA-binding IgG1 mAb, M9346A, conjugated to the potent microtubule inhibitor, soravtansine (DM4).[34] The ROR1-targeting ADC, VLS-101, consisting of the mAb, zilovertamab, conjugated via a linker to another microtubule cytotoxin, monomethyl auristatin E (MMAE), has been shown to have preclinical activity in Richter syndrome and CAR-T relapsed MCL.[35,36] A recent phase II clinical trial examined the activity of VLS-101 in solid cancers, including platinum-resistant OC (NCT04504916). The ROR1-targeting ADC, NBE-002 (also known as huXBR1-402-G2-PNU), which combines a humanised anti-human ROR1 mAb, huXBR1-402, linked to a payload of LC-G2-EDA-PNU, an anthracycline derivative of PNU-159682, has demonstrated significant activity in B-cell ALL, as well as MCL.[37] In this study, we investigated the activity of NBE-002 in preclinical models of HGSOC, both *in vitro* and *in vivo*.

Methodologies

The reporting of this study conforms to the ARRIVE (Animal Research: Reporting of In Vivo Experiments) guidelines 2.0[38] (Supplemental Table 1).

ROR1 ADCs construction

NBE-002 (huXBR1-402-G2-EDA-PNU) was generated as described.[39] NBE-002 and its isotype control ADC (Qb3-LC-G2-EDA-PNU) were diluted in phosphate-buffered saline (PBS). Stock solution was stored at −80°C and the working dilutions were prepared freshly. ADCs were prepared in a 3.5-fold serial dilution starting from 8 μg/mL. PA-1 was plated in 96-well plates and incubated with ADCs for 6 days. CellTiter-Glo cell viability assay (#G9243; Promega, Madison, Wisconsin, USA) was applied to assess the dose–response following the treatment of the ADCs.

Cell culture

The ovarian teratocarcinoma cell line PA-1 was cultured in MEM complete medium (supplemented with 10% foetal bovine serum, 1× GlutaMax and 1% Pen/Strep). HGSOC cell lines OVCAR4, Kuramochi, PEO1, PEO4 and OAW28 were cultured in RPMI complete medium. All cell lines were incubated at 37°C and 5% carbon dioxide, and were tested routinely for mycoplasma contamination.

PA-1 cell line xenograft model

Female NMRI-Foxn1nu (BomTac:NMRI-Foxn1nu) mice were purchased from Taconic, Denmark and allowed to acclimate for at least 5 days before the start of the experiments. All animals were housed in Macrolon® type III cages in groups of 8–10 animals under standardised conditions (21.5 ± 1.5°C temperature, 55% ± 10% humidity, 12 h light–dark cycles), and received a standardised diet (PROVIMI KLIBA) and autoclaved tap water ad libitum. Each animal was identified using subcutaneous microchips implanted under isoflurane anaesthesia. On the day of injection, PA-1 cells were harvested by centrifugation, washed and resuspended in 5% FBS (in PBS 1×) at a concentration of 1×10^8 cells/mL. The cell suspension was mixed at a 1:1 ratio with Matrigel (#356231; Corning, New York, USA) to obtain a final concentration of 5×10^7 cells/mL and 100 μL of the cell suspension was injected subcutaneously into the right flank of ~7-week-old mice. Tumour volumes (in mm^3) were determined three times a week via caliper measurements and the following formula: Tumour volume = length * width2 * π/6. Once tumours reached volumes of 117.18–226.82 mm^3, mice were randomly distributed across treatment and control groups by tumour size using the data storage system Sepia. Group sizes were determined by sample size calculation and animals were housed by treatment groups. All compounds and vehicle controls were administered i.v. at a volume of 5 mL/kg, by experimenters that were

not blinded to the treatment. To monitor treatment side effects, mice were inspected daily and body weight was measured thrice a week. Animals were euthanised by cervical dislocation when their tumours exceeded a volume of 1500 mm^3, in which case the tumour volume was carried forward in the analysis. In the experiment depicted in Figure 1(b)–(d), three animals reached humane endpoint prior to the end of the experiment (day 18): two animals in the isotype ctrl ADC, 0.11 mg/kg group (one emaciated mouse on day 14 and one mouse with a tumour volume >1500 mm^3 on day 16) and one animal in the isotype ctrl ADC, 0.33 mg/kg group (tumour volume >1500 mm^3 on day 16) had to be sacrificed. The lowest dose of NBE-002 was adjusted from 0.11 mg/kg (first experiment; Figure 1(b)–(d)) to 0.165 mg/kg (second experiment, Figure 1(e)–(i)) to directly

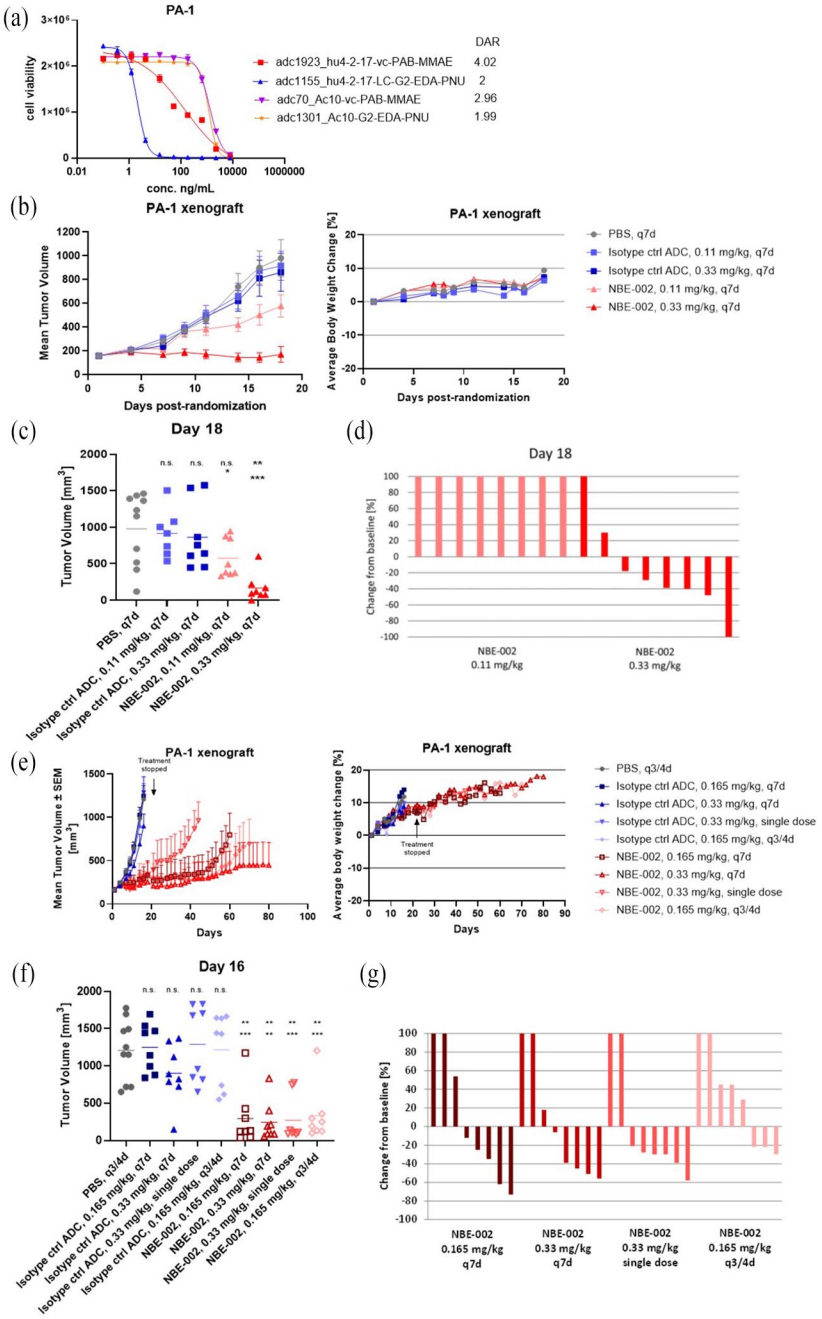

Figure 1. (Continued)

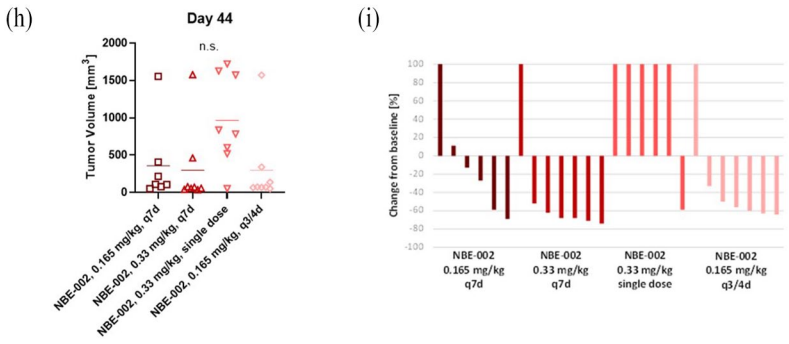

Figure 1. ROR1 ADC showed anti-tumour effects in ROR1-high PA-1 models. (a) Dose–response curves of PA-1 to a range of ROR1 ADCs at day 6. (b) Tumour growth (left panel; mean ± SEM) and average body weight change (right panel) of mice subcutaneously injected with the PA-1 ovarian teratocarcinoma cell line (xenograft) and treated with either NBE-002 or its isotype control ADC at the indicated doses and schedules. (c) Individual tumour volume in mm^3 on day 18 (last day of the experiment) and (d) Change from baseline (tumour volume on day 18 normalised to tumour volume at the start of treatment) from the experiment depicted in (c). Each dot or bar represents one animal; the horizontal lines in (d) represent the mean tumour volume. (e) Tumour growth (left panel; mean ± SEM) and average body weight change (right panel) of mice subcutaneously injected with the PA-1 ovarian teratocarcinoma cell line (xenograft) and treated with either NBE-002 or its isotype control ADC at the indicated doses and schedules. The last treatment was administered on day 22, after which tumour regrowth was monitored. (f) Individual tumour volume in mm^3 on day 16 (last day of the vehicle control group) and (g) change from baseline (tumour volume on day 16 normalised to tumour volume at the start of treatment) from the experiment depicted in (e). Each dot or bar represents one animal. (h) Individual tumour volume in mm^3 on day 44 (when the first NBE-002-treated group was stopped) and (i) change from baseline (tumour volume on day 44 normalised to tumour volume at the start of treatment) from the experiment depicted in (e). Each dot or bar represents one animal. The horizontal lines in (f) and (h) represent the mean tumour volume. One-sided non-parametric Mann–Whitney–Wilcoxon *U* tests with Bonferroni–Holm adjustments; for (c) and (f), top row: comparison to PBS control, bottom row: comparison to the respective isotype control groups. Change from baseline values is capped at 100%.
$^*p < 0.05$. $^{**}p < 0.01$. $^{***}p < 0.001$.
ADC, antibody–drug conjugate; n.s., non-significant ($p > 0.05$); PBS, phosphate-buffered saline; ROR1, tyrosine kinase-like orphan receptor 1.

compare the efficacy of the 0.33 mg/kg weekly dose administered according to two dose schedules: once and twice split-dose regimen per week. A 0.11 mg/kg dose given 3 times/week to maintain the same total weekly dose was deemed impractical due to potential stress on the animals. In Figure 1(e)–(i), tumour volume comparisons were performed on day 16, as the vehicle and isotype control groups had reached a humane endpoint by this time. Additionally, two animals had to be euthanised before the experiment endpoint in the NBE-002, 0.165 mg/kg, q7d group (one on day 25 due to body weight loss and one on day 39 due to tumour volume $>1500\,mm^3$), two in the NBE-002, 0.33 mg/kg, q7d group (one on day 42 and one on day 65 due to tumour volume $>1500\,mm^3$), two in the NBE-002, 0.33 mg/kg, single dose group (both on day 23 due to tumour volume $>1500\,mm^3$) and two in the NBE-002, 0.165 mg/kg, q3/4d group (one on day 23 and one on day 65 due to tumour volume $>1500\,mm^3$).

Ascites-derived primary cell lines

Four HGSOC patient ascites-derived cell lines (OC012, OC017, OC018 and OC023) were established following the procedure outlined in Shepherd et al.[40] In summary, the ascites fluid was transferred into the culture flasks with the addition of an equal volume of the complete RPMI medium. The medium was replenished every 3–4 days once most of the cells were established. Cells were trypsinised and passaged when confluent. Only early passages of the cells (less than four passages) were applied for cell assays to minimise the risk of morphological or other changes that may occur with prolonged passaging.

Western blot

Protein was extracted from the cell lines using cell lysis buffer (Cell Signalling Technology, Danvers, Massachusetts, USA) and supplemented with protease and phosphatase inhibitors (Cell

Signalling Technology, Danvers, Massachusetts, USA). The protein concentration was determined using the Pierce bicinchoninic acid assay kit (ThermoFisher Scientific, Waltham, Massachusetts, USA). Subsequently, Western Blot analysis was performed as previously outlined.41 Primary antibodies, specifically monoclonal rabbit anti-ROR1 (#AF2000; R&D Systems, Minneapolis, Minnesota, USA) and monoclonal mouse anti-α-Tubulin (#3873; Cell Signalling Technology, Danvers, Massachusetts, USA), were employed in this analysis.

ROR1 surface flow cytometry

Cell surface ROR1 levels on the HGSOC cells were assessed using flow cytometry. In brief, the cells were initially blocked with Human TruStain FcX (#422302; BioLegend, San Diego, California, USA) for 20 min at 4°C. Subsequently, they were incubated with either a PE anti-human ROR1 antibody (#357804; BioLegend, San Diego, California, USA) or an isotype control antibody (#400112; BioLegend, San Diego, California, USA) for 60 min at 4°C in the dark. Cell fluorescence of ROR1 (PE channel) was measured using the flow cytometer (BD FACSCanto II, BD Biosciences, San Jose, California, USA). BD Quantibrite beads (#340495; BD Biosciences, San Jose, California, USA) were run in parallel as internal standards to quantify the PE levels as per the manufacturer's protocol.

Dose–response assays

Cells were plated in 96-well plates within their specific media and incubated overnight. On the following day, cells were treated with NBE-002 using 1:2 serially diluted doses ranging from 0.1 to 20 μg/mL, or vehicle control (0.1% DMSO) in triplicates. Annexin V Red Dye at a dilution of 1:400 was also applied to stain apoptotic cells. Cell confluency and red fluorescent cells were monitored for a total period of 120 h in the IncuCyte S3 Live Imaging system (Sartorius, Goettingen, Germany). Both fluorescent and phase images were captured every 3 h at a 10× magnification. For each cell line, three independent tests, each with triplicates, were conducted. Cell confluence of each time point was normalised against the baseline. The relative cell apoptosis was calculated by dividing the red fluorescence area over the phase confluence area. A non-linear regression model was fit to estimate the half maximal inhibitory concentration (IC50) dose at 120 h.

Interactive analysis of combined treatments

To evaluate the combined effect of NBE-002 in conjunction with commonly used therapies, we subjected HGSOC cell lines (OVCAR4, Kuramochi, PEO1 and PEO4), along with a chemoresistant primary cell line (OC023), to various treatment conditions. Specifically, we treated these cells with different concentrations of NBE-002 (0.625, 1.25, 2.5, 5, 10 μg/mL) either alone or in combination with carboplatin (0, 3.125, 6.25, 12.5, 25, 50 μM), paclitaxel (0, 1.25, 2.5, 5, 10, 20 nM) or olaparib (0, 3.125, 6.25, 12.5, 25, 50 μM). SynergyFinder 2.0[42] was applied to visualise and estimate the combination effects, employing the Bliss independence model to calculate combination factors.

ROR1 immunohistochemistry

Formalin-fixed paraffin-embedded PDX tumour samples were sectioned and automated immunohistochemistry was performed on the BOND RX (Leica Biosystems, Nussloch, Germany) with anti-ROR1 antibody.[17] IHC slides were scanned digitally at 20× magnification using the Pannoramic Scan II scanner (3DHISTECH Ltd., Budapest, Hungary) and high-definition images were uploaded into CaseCenter (3DHISTECH Ltd., Budapest, Hungary). Membranous ROR1 staining was scored by a gynaecological pathologist and an *H*-score was determined; *H*-score = (%strong positive × 3) + (%moderate positive × 2) + (%weak positive × 1).

PDX generation and in vivo treatment

All animal research was performed according to the Australian Code for the Care and Use of Animals for Scientific Purposes 8th Edition, 2013 (updated 2021) and was approved by the WEHI Animal Ethics Committee (2019.024 and 2022.030).

Female NSG (NOD-*scid* IL2Rg^{null}) mice 6–10 weeks of age were obtained from the WEHI-specific pathogen-free breeding facility and allowed to acclimate for at least 3 days before the start of the experiments. Animals were housed in Tecniplast Emerald IVC enclosures under standard conditions (21 ± 3°C temperature, 55% ± 15% humidity, 14 h/10 h light–dark cycles). Each animal was identified using subcutaneous microchips implanted under isoflurane anaesthesia.

The following HGSOC PDX models have been described previously: #56, #62, #201,[43] #32, #111, #931[44] and #56 pp.[45] PDX models #22, #419 and #448 were generated from fresh biopsy or surgical specimens, which were cut into small fragments and transplanted subcutaneously on the flank of NSG mice.[43] PDX models were validated by histological review, conducted by a gynaecological pathologist, and by BROCA panel sequencing (mutation match with patient sample). Relevant clinical data and key molecular features are presented in Supplemental Table 2.

Reagents for *in vivo* treatments were human immunoglobulin (also known as IVIg; Privigen; CSL Behring, Parkville, Victoria, Australia), NBE-002, Qb3-LC-G2-EDA-PNU (referred to as isotype control; anti-Qb3 antibody recognises a bacteriophage Qβ protein), carboplatin (Pfizer, New York City, New York, USA) and olaparib (MedChemExpress, Monmouth Junction, New Jersey, USA). Olaparib was prepared in 10% DMSO and 10% hydroxypropyl-β-cyclodextrin. The vehicle for all other treatments was Dulbecco's phosphate-buffered saline (DPBS). NSG mice bearing passage 5–9 tumours (180–300 mm^3 in size) were randomly assigned to the following treatment regimens, weekly cycles for 4 weeks. Rolling enrolment was used, with mice being assigned equally across the treatment arms as tumours reached the treatment volume. Tumour measurement, randomisation and treatments were each performed by separate researchers or technicians, with technicians blinded to the study hypothesis, design and data analysis. Studylog software (Studylog Systems Inc., San Diego, California, USA) was used to record and track tumour volume and Animal Management System software (WEHI, Melbourne, Victoria, Australia) to manage animal procedures and ethics.

1. IVIG day 1 (30 mg/kg, IV) + DPBS day 2
2. IVIG day 1 (30 mg/kg, IV) + Isotype control day 2 (0.33 mg/kg, IV)
3. IVIG day 1 (30 mg/kg, IV) + NBE-002 day 2 (0.33 mg/kg, IV)
4. IVIG day 1 (30 mg/kg, IV) + Isotype control day 2 (0.33 mg/kg, IV) + carboplatin day 2 (50 mg/kg, IP)
5. IVIG day 1 (30 mg/kg, IV) + NBE-002 day 2 (0.33 mg/kg, IV) + carboplatin day 2 (50 mg/kg, IP)
6. IVIG day 1 (30 mg/kg, IV) + Isotype control day 2 (0.33 mg/kg, IV) + olaparib daily (100 mg/kg, oral gavage)
7. IVIG day 1 (30 mg/kg, IV) + NBE-002 day 2 (0.33 mg/kg, IV) + olaparib daily (100 mg/kg, oral gavage)
8. Carboplatin d1 (50 mg/kg, IP)

Digital calliper tumour measurements were taken twice weekly until tumour volume reached >700 mm^3 (humane endpoint for tumour volume, 1000 mm^3) or mice reached the experimental endpoint, 120 days post-treatment. Additionally, humane endpoints were reached for 10 mice that were assessed by a veterinarian. Mice were euthanised and post-mortems were conducted: three mice had thymic lymphomas (days 35, 88 and 108 from the start of treatment), which are known to occur occasionally in NSG mice; one mouse had an ulcerated tumour (day 43); three mice had weight loss that reached humane endpoint (−20%; days 9, 63, 84) and three mice were hunched and appeared unwell but post-mortem did not identify a cause (days 31, 108 and 134). Five mice with weight loss or that were hunched were on a carboplatin treatment regimen, one mouse single agent carboplatin, three mice isotype control + carboplatin and one mouse NBE-002 + carboplatin. One mouse with weight loss received NBE-002 + olaparib treatment. These events are censored on the Kaplan–Meier survival curves as the tumour volume endpoint was not reached.

Statistical analysis

One-tailed non-parametric Mann–Whitney–Wilcoxon *U* test was performed to compare the effect of the treatments on the vehicle control group, as well as to compare the effect of each dose and schedule of NBE-002 to its respective isotype control ADC treatment group in the PA-1 xenograft models. Within each subtopic, the *p* values of the efficacy parameters were adjusted for multiple comparisons according to Bonferroni–Holm. Group analysis was stopped when <70% of the animals within the group remained and curves were truncated on the graphs past those timepoints (in Figure 2 on day 60 for the NBE-002, 0.165 mg/kg, q7d group, on day 44 for the NBE-002, 0.33 mg/kg, single dose group and on day 70 for the 0.165 mg/kg, q3/4d group). Two-way ANOVA (time and treatment as factors) was performed to compare cell

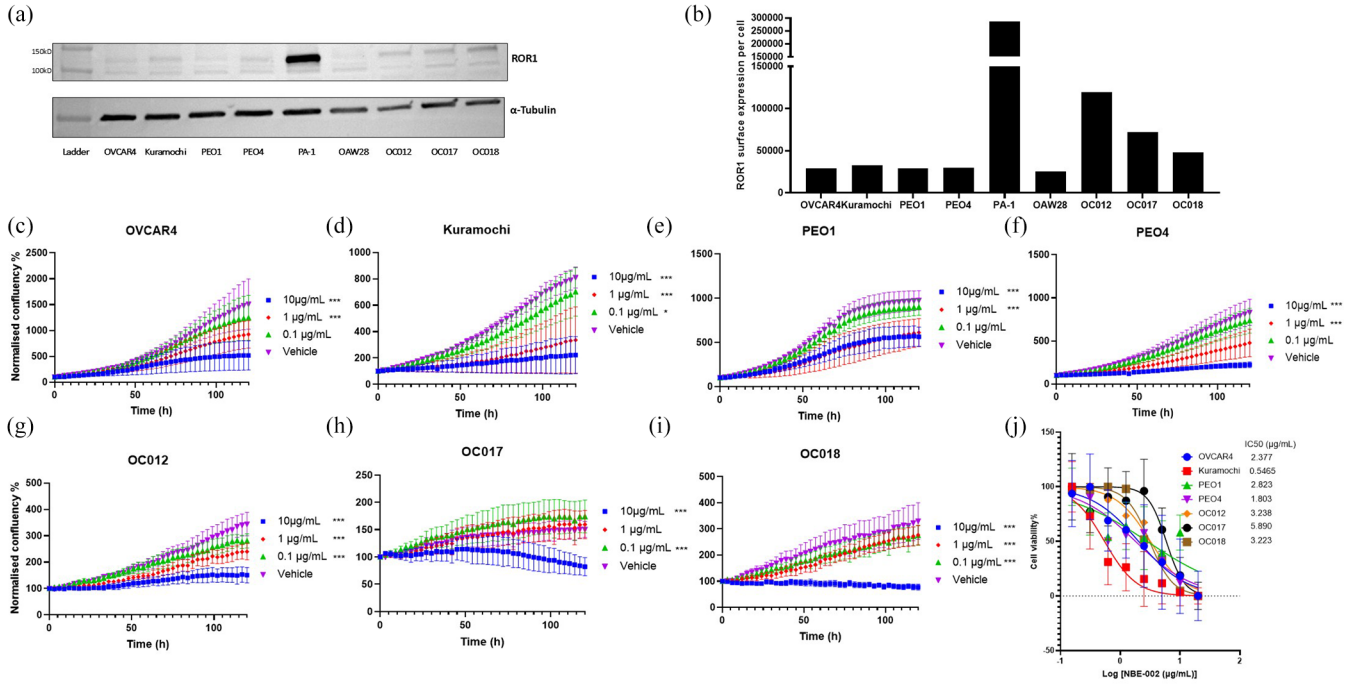

Figure 2. NBE-002 treatment inhibited the growth of ROR1-expressing HGSOC cell lines *in vitro*. (a) Western blot of ROR1 (Polyclonal Goat IgG, R&D systems, AF2,000) in HGSOC cell lines, as well as high and low ROR1 expressed control cell lines PA-1 and OAW28. (b) Cell surface ROR1 expression level of the cell lines was analysed with PE anti-ROR1 antibody (BioLegend, clone 2A2) using BD Quantibrite Beads. (c)–(i) Cell confluency of the HGSOC cell lines following ROR1 ADC treatment by IncuCyte S3 imaging for a total period of 120 h. Two-way ANOVA (time and treatment as two factors) was performed to assess the mean differences of cell confluency across treatments, with Tukey's multiple comparison test used to adjust the *p* value. (j) Dose–response curves and IC50 of NBE-002 at 120 h. For panels (c)–(j), $n = 3$, the error bar represents the standard deviation.
*Adjusted $p < 0.05$. ***Adjusted $p < 0.001$.
ADC, antibody–drug conjugate; HGSOC, high-grade serous ovarian cancer; n.s., non-significant ($p > 0.05$); PBS, phosphate-buffered saline; ROR1, tyrosine kinase-like orphan receptor 1.

confluence or tumour growth between various treatments. Post hoc Tukey tests were applied to correct for multiple comparisons. Kaplan–Meier survival analysis (with tumour volume at the endpoint) was performed using the log-rank test. Statistical analysis and figure generation were carried out using GraphPad Prism (v10.2.0; GraphPad Software, San Diego, California, USA). Statistical significance representations: $*p < 0.05$, $**p < 0.01$, $***p < 0.001$. Data were presented as mean ± standard deviation.

Results

Single-agent NBE-002 was active even at a low dose in vitro and in vivo in ROR-high expressing preclinical models

We constructed a range of ROR1 ADCs, with different ROR1-targeting antibodies and payloads, (DAR shown in Figure 1(a)). The effects of the ADCs were evaluated using the high ROR1-expressing ovarian teratocarcinoma cell line, PA-1. ROR1 ADCs (adc1923, adc1155) exhibited a higher level of sensitivity than did their corresponding isotype control mAbs targeting CD30 (Figure 1(a)). Notably, adc1155, with the LC-G2-EDA-PNU payload, exhibited greater activity than adc1923, which had a vc-PAB-MMAE payload. Consequently, adc1155, referred to as NBE-002 henceforth, was selected for subsequent downstream analysis. In the PA-1 xenograft model, NBE-002 administered at 0.11 or 0.33 mg/kg every 7 days (q7d) significantly suppressed the tumour growth at day 18 relative to the respective isotype control ADC groups (Figure 1(b)–(d), $p = 0.02$ and 0.0003, respectively). Additionally, no average body weight loss was observed in any of the treatment groups (Figure 1(b), right panel). In the same PA-1 xenograft model, the efficacy of NBE-002 with 0.33 mg/kg weekly dose was assessed according to two dose schedules. Mice received 0.33 mg/kg either as a single dose or repeated once a week

(q7d x3) or 0.165 mg/kg, either as a single dose or repeated twice a week (q3/4d x3). All tested dosing regimens resulted in a significant inhibition of tumour growth when compared to the vehicle control or the corresponding isotype control ADC (at day 16; Figure 1(e)–(g)). Following treatment discontinuation, the most prolonged response across all tested doses and schedules was observed in the animal group which received 0.33 mg/kg NBE-002 on a once weekly schedule. The responses were sustained overtime (at day 44; Figure 1(h) and (i)).

Single-agent NBE-002 treatment inhibited HGSOC cell growth in vitro across a range of HGSOC cell lines

ROR1 expression was profiled in the HGSOC cell lines, OVCAR4, Kuramochi, PEO1, PEO4. Derived from the same *BRCA2*-mutated HGSOC, from samples collected at different times in the patient trajectory, PEO1 is chemosensitive and HRD, whilst PEO4 is chemoresistant and HRP, due to treatment pressure resulting in a secondary *BRCA2* reversion mutation. In addition, three HGSOC cell lines, OC012, OC017 and OC018, were established from patient ascites fluid and also used for subsequent experiments. Patient clinicopathological characteristics are summarised in Supplemental Table 3. The ovarian teratocarcinoma cell line PA-1 and the HGSOC cell line OAW28 were included as ROR1 high and low controls, respectively. Most of the HGSOC cell lines exhibited a moderate to low level of ROR1 expression (Figure 2(a) and (b)). Notably, the more recently derived OC cell lines demonstrated higher levels of ROR1 expression in terms of surface and total protein, compared with long-established commercial cell lines. Subsequently, we monitored the real-time growth of four HGSOC cell lines (OVCAR4, Kuramochi, PEO1, PEO4) as well as three cell lines recently derived from ascites (OC012, OC017 and OC018), following treatment with NBE-002 by IncuCyte S3 platform imaging for a total period of 120 h (Figure 2(c)–(i)). Treatment with NBE-002 at doses of 1 and 10 μg/mL significantly inhibited cell growth in all cell lines, except for OC017. Notably, for Kuramochi and ascites cell lines OC012, a dose of NBE-002 as low as 0.1 μg/ml was sufficient to significantly suppress cell growth. Commercial cell lines exhibited a lower IC50 compared with more recently derived ascites cell lines (1.89 ± 0.99 vs 4.1 ± 1.53 μg/mL, Figure 2(j), relevant p values included).

Single-agent NBE-002 treatment induced apoptosis in HGSOC cell lines

To investigate apoptosis following NBE-002 treatment, cells were incubated with Annexin V red dye (Sartorius, Goettingen, Germany) during the IncuCyte run. A significantly higher number of red-stained cells, indicative of apoptosis, was observed in HGSOC cell lines when exposed to NBE-002 at doses ranging from 0.1 to 10 μg/mL (Figure 3(a)–(n), relevant p values included). At the 10 μg/mL dose, a significant portion of cells had detached and displayed red staining in all cell lines tested; these cells are not included in the IncuCyte analysis. Kuramochi, the cell line exhibiting the highest sensitivity based on the IC50 (Figure 2(j)), demonstrated a substantial induction of apoptosis from the start of treatment (1 h prior to the beginning of the IncuCyte run), with cells detaching from the plate at the 0.1 μg/mL NBE-002 dose (Figure 3(d)).

NBE-002 was synergistic in combination with SoC therapies in HGSOC cell lines

To assess the combination effect of NBE-002 with SoC therapies used in the clinic, we applied the Bliss model within the SynergyFinder 2.0 tool to estimate combinatorial effects (Figure 4). Since most of the ascites-derived cell lines were nearly depleted in earlier experiments, we substituted a fourth cell line, derived from a chemo-resistant HGSOC patient with ROR1 expression, in the combination analysis. A synergistic effect was observed when NBE-002 was combined with carboplatin in two out of five cell lines (PEO4 and OC023, chemo-resistant), and when NBE-002 was combined with the PARPi, olaparib, in one out of five cell lines (PEO1, BRCA2 mutated, HR deficient). No synergy was observed for NBE-002 in combination with paclitaxel in any cell line. For the majority of cell lines, combining NBE-002 with SoC therapies showed an additive effect: three out of five cell lines for NBE-002 and carboplatin combination, four out of five for NBE-002 and paclitaxel combination and four out of five for NBE-002 and olaparib combination.

The activity of NBE-002 in HGSOC PDX models was dependent on ROR1 expression level and HR status

ROR1 expression was assessed in 26 PDX models of HGSOC (Supplemental Table 2). These PDX models cover the major contexts of the HGSOC patient journey, from chemo-naïve, to

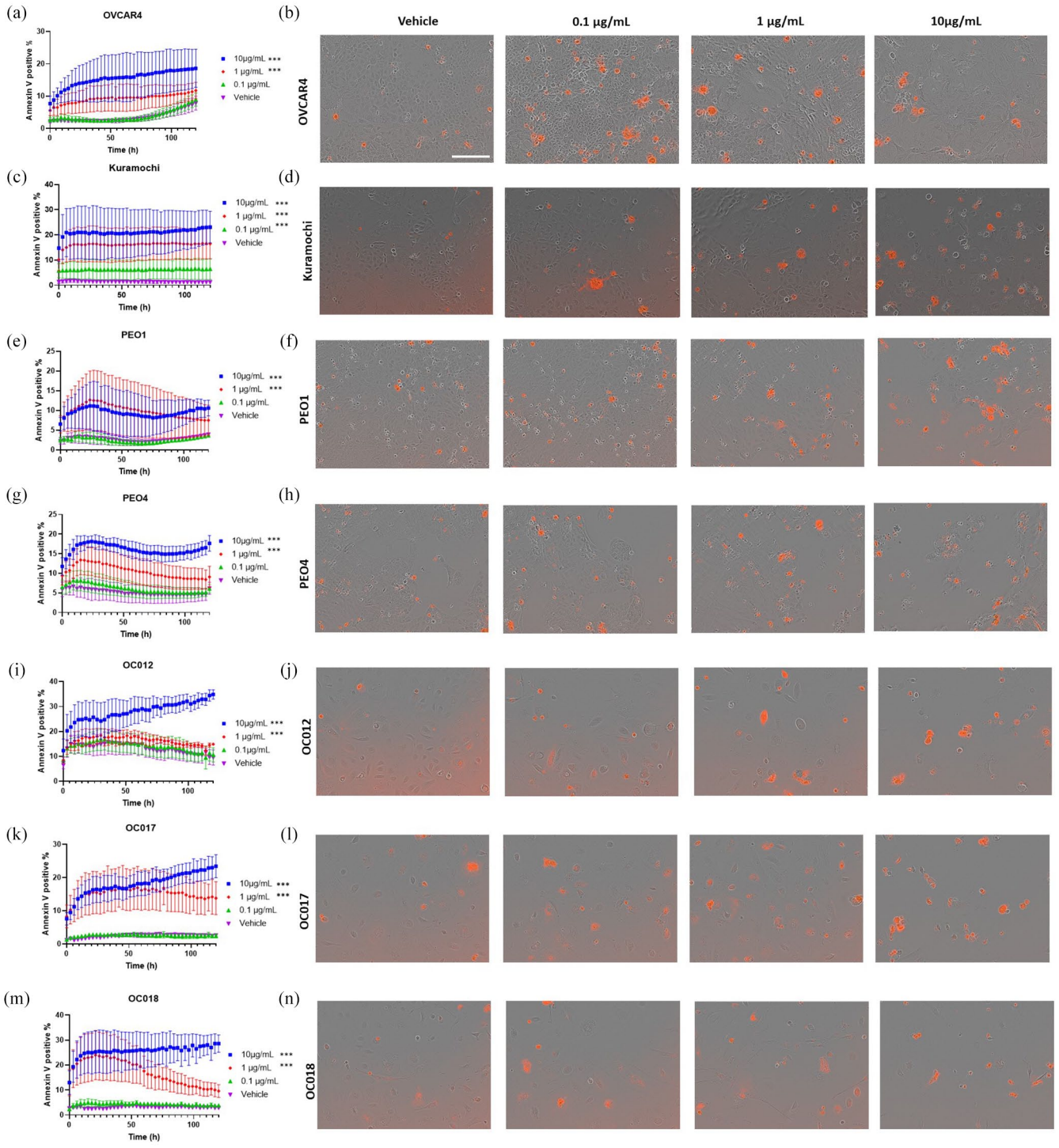

Figure 3. NBE-002 induced apoptosis of HGSOC cell lines *in vitro*. Figures (a), (c), (e), (g), (i), (k) and (m) displayed a red Annexin V positive proportion of HGSOC cell lines over time when incubated with NBE-002 or vehicle control ($n = 3$ independent experiments), as detected by the IncuCyte S3 platform. Figures (b), (d), (f), (h), (j), (l) and (n) include representative images captured by the IncuCyte at 120 h, scale bar 200 μm, magnification 10×. The images were selected from one of the three independent experiments. Two-way ANOVA (time and treatment as two factors) was performed to assess the mean differences of cell apoptosis% across treatments, with Tukey's multiple comparison test used to adjust the *p* value.
*$p < 0.05$. **$p < 0.01$. ***$p < 0.001$.
HGSOC, high-grade serous ovarian cancer.

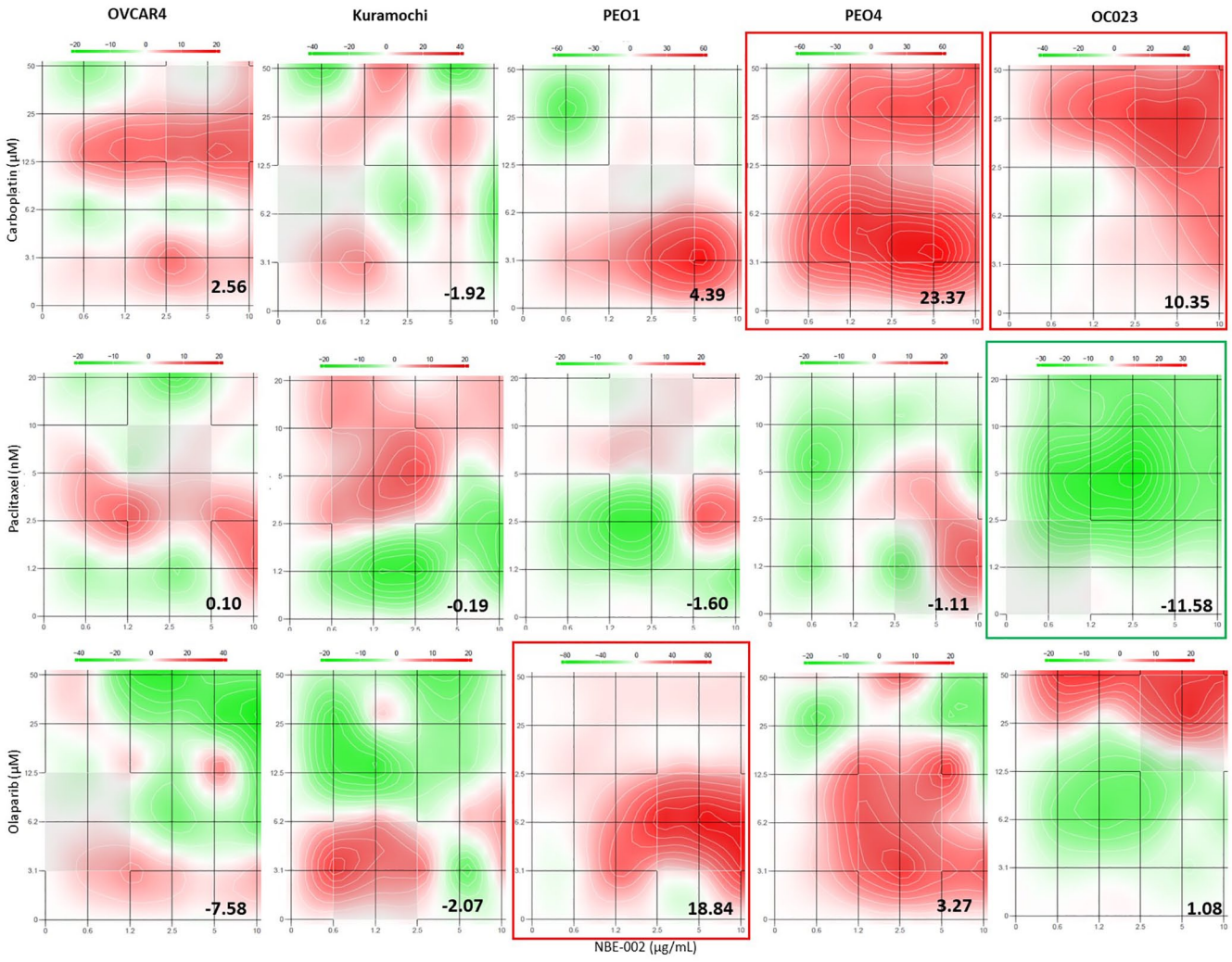

Figure 4. Analysis of interactions between NBE-002 and standard-of-care therapies in high-grade serous ovarian cancer cell lines at 120 h. Dose–response matrices with Bliss synergy scores (values located in the bottom right corner of each panel) estimated via SynergyFinder indicated synergistic (>10, highlighted in red), subadditive (<−10, highlighted in green) or additive (−10–10) effect of the drug combination.

post-chemotherapy (following a range of numbers of lines (1–7 lines)) and post-PARPi; as well as covering the major molecular categories relevant for the clinic: HRP, HR deficient and HR reversion, having originally been HRD. ROR1 expression was scored by a pathologist, from absent to high expression (0–3) and the percentage of the corresponding tumour area was estimated. *H*-scores were derived, with scores ranging from 0 to 285 being observed; with more than half of the 26 distinct PDX models (62%) having low expression with an *H*-score <100 (median *H*-score 86.5). Chemo-naïve PDX models had a numerically greater representation in the ROR1 medium-to-high expression group: *H*-score >100, 5 out of 10 chemo-naïve (50%) versus *H*-score <100, 5 out of 16 chemo-naïve (31%). Five out of seven (71%) functionally HRD models (i.e. those models that were responsive to PARPi treatment, as well as being molecularly consistent with HRD), had a ROR1 *H*-score >100; conversely, only one of eight (12.5%) post-PARPi HRD reversion to HRP PARPi-resistant models had a ROR1 *H*-score >100 (Chi-square test $p = 0.02$). Therefore, it appeared that ROR1 expression likely decreased with disease progression. This was supported by a matched PDX pair #56 (*H*-score 190) and #56pp (*H*-score 83), generated from chemo-naïve and post-PARPi samples, respectively, collected 7 years and five lines of treatment apart, from the same patient.

Ten PDX models with a range of ROR1 IHC intensity and known HRP or HRD status were selected for *in vivo* investigation (Figure S1). The number of PDX models and the body weights of each experimental group are shown in Supplemental Tables 4, 5 and Figure S2, respectively. As NOD-*scid* IL2Rg^{null} (NSG) mice are highly immunodeficient and lack production of immunoglobulin, 24 h prior to treatment with NBE-002, immunoglobulin (Ig) was administered to block Fc receptors. This step reduced the Fc-mediated binding of NBE-002, or any ADC, to myeloid cells in nontarget organs.[46] NBE-002 significantly suppressed tumour growth and improved OS in the ROR1 high HRD model PDX#62 (ROR1 *H*-score 178), compared with the mAb isotype control treatment (Figure 5(a) and (k); Supplemental Tables 4 and 5). Single-agent NBE-002 treatment suppressed tumour growth of PDX#56 (ROR1 *H*-score 190, HRD) and PDX#22 (ROR1 *H*-score 90, HRD reversion) without improving survival compared to the isotype control, which had activity in these models (Figure 5(b), (f) and (k); Supplemental Tables 4 and 5). The combination of NBE-002 with carboplatin resulted in a greater reduction in tumour

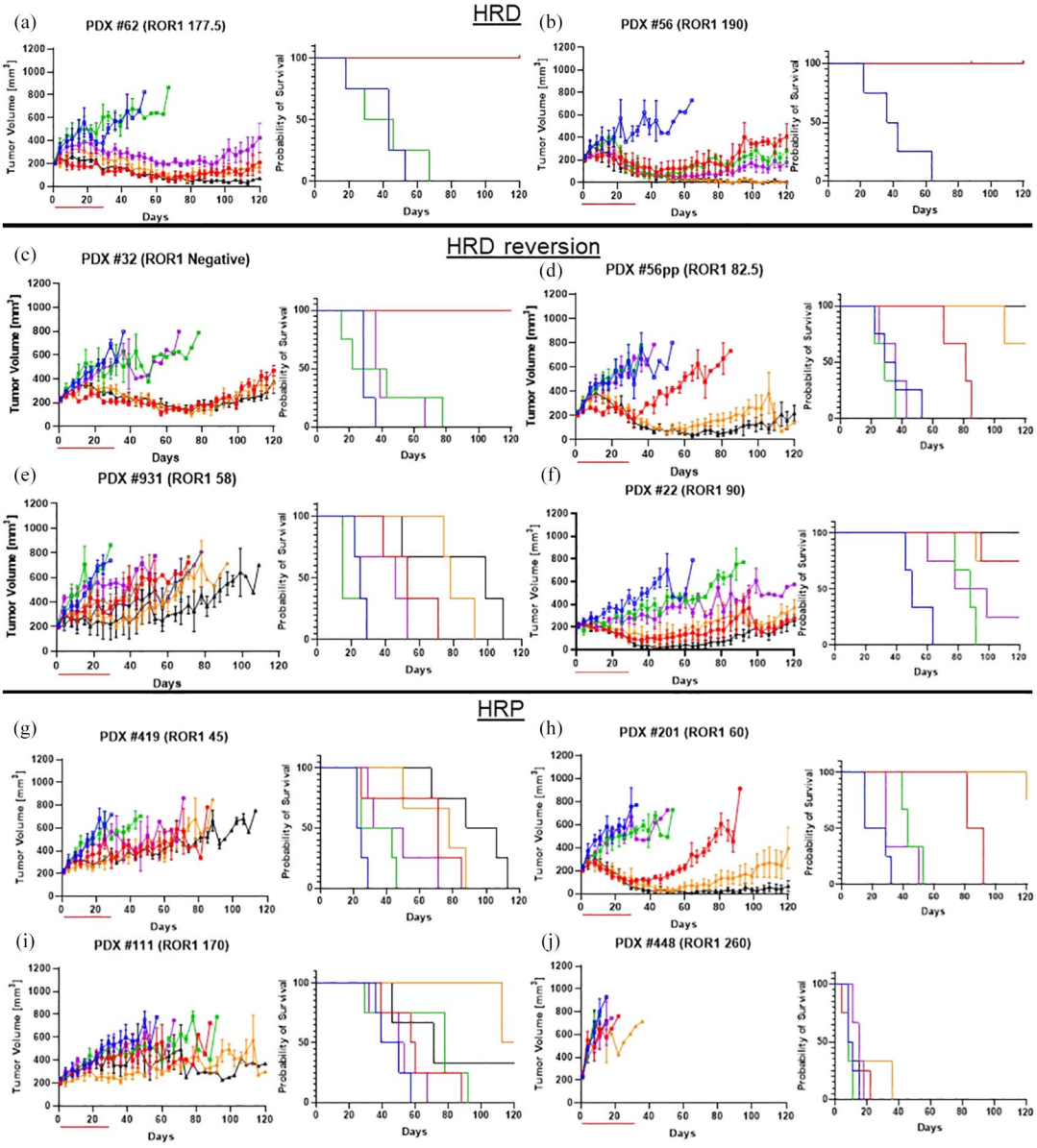

Figure 5. (Continued)

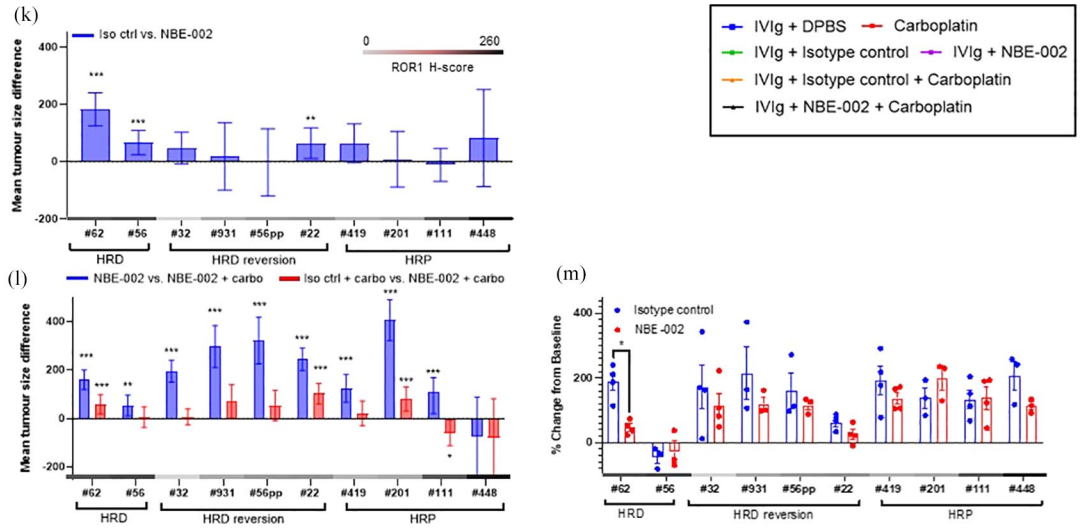

Figure 5. NBE-002 inhibited tumour growth as a single agent in ROR1-high HRD and post-HRD reversion PDX models and combination with carboplatin. (a–j) Tumour volume (left, mean ± SEM) and Kaplan–Meier survival curves (right) for in vivo PDX treatments ((a–b) for HRD models, (c–f) for HRD reversion models, (g–j) for HRP models). The ROR1 *H*-score is shown in each panel adjacent to the PDX ID. Mice were treated for 4 weeks with weekly cycles of: IVIg (30 mg/kg) day 1 + DPBS day 2, IVIg (30 mg/kg) day 1 + Isotype control (0.33 mg/kg) day 2, IVIg (30 mg/kg) day 1 + NBE-002 (0.33 mg/kg) day 2, IVIg (30 mg/kg) day 1 + Isotype control (0.33 mg/kg) day 2 + carboplatin (50 mg/kg) day 2, IVIg (30 mg/kg) day 1 + NBE-002 (0.33 mg/kg) day 2 + carboplatin (50 mg/kg) day 2, IVIg (30 mg/kg) day 1 + Isotype control (0.33 mg/kg) day 2 or carboplatin (50 mg/kg) q7d. The PDX models #56 and #56pp (pp: post-PARPi) were a matched PDX pair from the same individual: #56 derived from a chemo-naïve sample and #56pp derived from a sample collected after multiple lines of treatment, including PARP inhibitor. The red bar below the *x*-axis indicates the treatment interval. For *n* per treatment arm and Kaplan–Meier Log-Rank analysis *p* values, see Supplemental Table 5. (k, l) The mean difference in tumour growth between treatments. Two-way ANOVA (time and treatment as two factors) was performed to assess the mean differences in tumour volume across treatments, with Tukey's multiple comparison test used to adjust the *p* value (Supplemental Table 4). (m) Percentage change in tumour volume from baseline for NBE-002 and isotype control-treated tumours at day 28, end of treatment (or earlier for rapidly growing PDX models).
$^{*}p < 0.05$. $^{**}p < 0.01$. $^{***}p < 0.001$.
DPBS, Dulbecco's phosphate-buffered saline; HRD, homologous recombination DNA repair deficient; HRP, HR proficient; PARPi, poly-(ADP-ribose) polymerase inhibitors; PDX, patient-derived xenograft; ROR1, tyrosine kinase-like orphan receptor 1.

volumes for PDX#62, 931, 22 and 201 compared with treatment with either isotype control plus carboplatin or NBE-002 (Figure 5(l)). In comparison to either single-agent carboplatin or NBE-002, PDX#56 and 56pp also showed combinatorial activity for NBE-002 delivered together with carboplatin (Figure 5(b) and (e); Supplemental Table 4).

Apart from two ROR1-high PDX models that were resistant to all treatments, PDX #111 and #448, the response to single-agent NBE-002 correlated with ROR1 expression #56 > #62 > #22. For models with lower ROR1 expression, such as #201 (*H*-score 60) and #56pp (*H*-score 83), no single-agent NBE-002 activity was observed. However, synergy in combination with carboplatin suggested that these models were not completely resistant to PNU, perhaps due to a lower dose/delivery of NBE-002, indicating the expression of ROR1 was not high enough for single-agent activity. As PDX #62 and #56 were sensitive to both NBE-002 and carboplatin as single agents, lower doses of each agent would need to be explored to uncover the full potential of this combination. In both PDX, however, the combination of NBE-002 and carboplatin was the most active treatment (Supplemental Tables 4 and 5).

Response to the isotype control ADC (the treatment arm of IVIg plus isotype control) was seen in 2 out of 10 PDX: in PDX #56 (ROR1 *H* score 190) but not #56pp (ROR1 *H* score 83) and in PDX #22 (ROR1 *H* score 90) and was unexpected. Perhaps as PDX #56 is very sensitive to all therapies, in keeping with the very long time

for the patient, from first diagnosis to ultimate PD on PARPi (3 years), following which she retained platinum sensitivity (another 2 years), lowering the dose of NBE-002 and of the isotype control might have revealed the specific ROR1-targeted response. Similarly, the isotype control + carboplatin arm responded better than did the carboplatin-alone arm in 4 out of 10 PDX, spanning the full range of carboplatin response-sensitive, mid-responsive and refractory. Despite this apparent increased sensitivity to carboplatin in the setting of isotype control, it was clear that the combination of NBE-002 and carboplatin was the best or equal to the best therapeutic arm in all 10 PDX.

Additionally, we explored the combination effect of NBE-002 with olaparib in two PDX models #62 and #931 representing HRD and HRD reversion. Combining NBE-002 with olaparib led to a decreased tumour size in the HRD model PDX #62 compared with treatment with either the isotype control plus olaparib or with NBE-002 ($p < 0.001$), albeit without a significant enhancement in survival compared with either monotherapy, as all mice survived until the experimental endpoint (120 days; Figure 6 and Supplemental Table 5).

Discussion

The high relapse rate of HGSOC has prompted the exploration of novel approaches to therapies, including in combination regimens. Targeted therapies have offered a promising solution by focusing on specific mechanisms or pathways, either associated with an Achilles' heel, such as the predicted synthetic lethality observed for PARPi in HRD OC or with resistance to standard chemotherapy. One of the challenges associated with targeted therapies involves the need for predictive biomarkers to identify the population most likely to benefit. The ADC class of drugs selectively deliver cytotoxic payload to malignant cells expressing a specific antigen, which reduces toxicity while enhancing efficacy via their targeting capability. ADC technology has evolved from chimeric antibodies and unstable linkers causing off-target toxicity to more effective humanised antibodies with stable linkers that enhance the specificity of drug release. To date, more than 10 ADCs have been approved by the FDA to treat numerous malignancies, with hundreds more being investigated in various stages of clinical trials.[47]

We have identified a clear target, ROR1, in HGSOC. Therefore, we conducted the first investigation into the effect of ROR1 ADC in HGSOC. We examined two different payloads (PNU and MMAE) for the ADCs. MMAE has been broadly applied in ADCs including the ROR1 targeting VLS-101. NBE-002 which contains the LC-G2-EDA-PNU payload, outperformed the ADC with vc-PAB-MMAE in prior work. Additionally, NBE-002 demonstrated specific activity in the ROR1 high PA-1 model both *in vitro* and *in vivo*. For clinical applications of NBE-002, we then analysed the surface ROR1 expression in HGSOC. ROR1 is expressed predominantly in either 105 or 130 kDa variant, with the unglycosylated isoform (105 kDa) correlated with more non-progressive pathology in CLL patients.[48] We observed two protein variants of ROR1 sized at 105 and 130 kDa, respectively, in HGSOC models. Through flow cytometry analysis, we found the glycosylated ROR1 (130 kDa) was the main form exposed on the cell surface in HGSOC cells, the same as previously reported for CLL.[49]

Single-agent NBE-002 treatment induced a potent cytotoxicity in ROR1 expressing HGSOC cell lines *in vitro*, with relatively low IC50s of ~6 µg/ml. Notably, Kuramochi cells, which exhibited the highest ROR1 expression among the four commercial HGSOC cell lines tested, demonstrated the greatest sensitivity to NBE-002 and a rapid apoptotic response (15% of cells underwent apoptosis within 1 h of treatment). This suggested a strong dependence on ROR1 expression for ADC-mediated cytotoxicity. Newly derived HGSOC cell lines with higher ROR1 expression levels, in fact, showed higher IC50 values to ROR1 ADC compared to commercial cell lines. However, it is important to note that commercial cell lines, which have been in culture for longer than more recently derived cell lines, may have developed additional changes, which is why the recently generated cell line and PDX preclinical models are so important. Notably, we observed significantly lower IC50 values for NBE-002 in the ascites-derived PEO1 and PEO4 compared to recently derived cell lines from ascites in this study. Additionally, more apoptosis events were observed in NBE-002-treated HGSOC cell lines compared to the vehicle control, indicating effective payload release into the cells.

In terms of the PDX models, the greatest single-agent NBE-002 activity was observed in

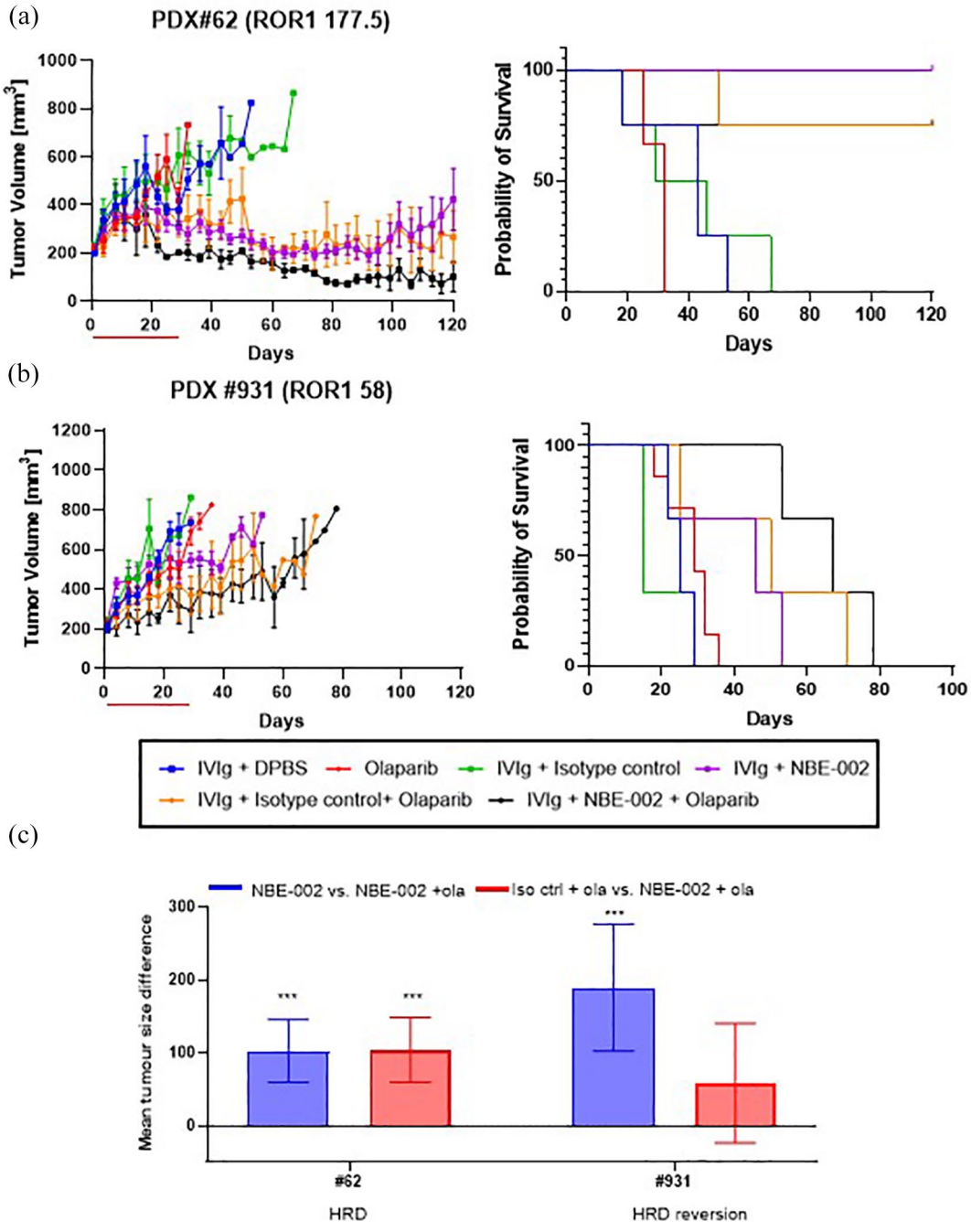

Figure 6. A combination effect was observed in an HRD model *in vivo* upon treatment with NBE-002 and olaparib. (a, b) Tumour volume (left, mean ± SEM) and Kaplan–Meier survival curves (right) for HRD PDX #62 (a) and HRD reversion PDX #931 (b). ROR1 *H*-score is shown in each panel next to the PDX ID. (c) The mean difference in the tumour growth between treatments. Two-way ANOVA (time and treatment as two factors) was performed to assess the mean differences in tumour volume across treatments, with Tukey's multiple comparison test used to adjust the *p* value (Supplemental Table 4). For *n* and Kaplan–Meier log-rank analysis *p* values, see Supplemental Table 5.
***$p < 0.001$.
HRD, homologous recombination DNA repair deficient; PDX, patient-derived xenograft; ROR1, tyrosine kinase-like orphan receptor 1.

ROR1-high HRD models. This is not surprising as in addition to high ROR1 expression, these models were derived from chemo-naïve patient samples that were also sensitive to platinum treatment. In HRD reversion HRP models, single-agent activity was observed in the PDX model with the highest ROR1 expression, #22. It should be noted that we used an isotype control ADC which linked the payload to an antibody targeting Qb3 to test the specificity of the NBE-002. We observed some cytotoxic effects introduced by the isotype control, most notably in PDX#56, suggesting potential non-specific interactions of the Qb3 isotype control ADC with some tumours, which could have been addressed by detailed dose-finding studies in each PDX (which is not feasible with *in vivo* models). ROR1 expression was extremely high in PA-1 compared to the HGSOC cell lines and PDX models, allowing for a lower effective dose of NBE-002 without significant effects being observed from the isotype control. In the HGSOC PDX studies, ROR1 expression or antibody affinity might be insufficient to demonstrate a differential response at the doses, except for PDX #62.

Prior clinical findings suggest that targeting a single pathway may not be adequate, and the effectiveness of combined therapies is impressive in many contexts across cancer types. As a result, we investigated NBE-002 in combination with SoC therapies. A synergistic effect was observed when NBE-002 was combined with carboplatin in the chemo-resistant cell lines, PEO4 and OC023 *in vitro*. The PEO4 cell line was derived from the same patient as PEO1 but after the development of resistance to platinum-based treatment and restoring HRP via a BRCA2 reversion mutation. The addition of NBE-002 sensitises the PEO4 cells to platinum treatment, highlighting its potential clinical significance for platinum-resistant HRP reversion HGSOC patients. In addition, the combination effect was significant in ROR1-positive platinum-responsive PDX models *in vivo*, when NBE-002 was combined with carboplatin, or in two out of two ROR1-positive HRD models when combined with the PARPi, olaparib. The combination of carboplatin with an anthracycline, typically with pegylated liposomal doxorubicin (PLD) is effective as second-line therapy in platinum-sensitive relapsed OC.[50] Our results with NBE-002 (anthracycline payload) and carboplatin in ROR1-positive PDX models are consistent with this. The combination effect was most evident in two models, #201 and #55PP, with low ROR1 expression and no single-agent NBE-002 activity; this suggested that even lower doses of NBE-002 (<0.33 mg/kg in this study) could be tested in ROR1-high PDX models, to demonstrate the potential of carboplatin combinatorial activity, an approach which could improve overall tolerability in the clinic. Notably, five of the PDX models used in this study had been generated from patients with prior PLD treatment: #32, #419, #931, #111 and #56pp (Supplemental Table 2). Mechanisms of anthracycline resistance may have developed and could explain the minimal/lack of combination activity in PDX #931 and #111, potentially also #32 and #419 although ROR1 expression was low in those models. We have also profiled the expression of the *ABCB1* gene (encoding multidrug resistance protein 1 or p-glycoprotein 1) in 7 out of 10 PDX, including #931, #111, #32 and #448. Only #448 exhibited high *ABCB1*[44] and unpublished data.

Conclusion

In conclusion, we have demonstrated that the ROR1 targeting ADC, NBE-002, has activity in ROR1-expressing HGSOCs, *in vitro*, as well as in 3 out of 10 HGSOC PDX models, predominantly those derived from patients who were earlier during the patient journey, with platinum-sensitive and HRD OC. This was in keeping with the response we saw in one out of two HRD PDX, for NBE-002 in combination with PARPi. Encouragingly, activity was also noted in six out of eight platinum-resistant/refractory PDX, in combination with carboplatin. These data support the clinical development of ADCs targeting ROR1 in combination with SOC therapies in ROR1 high HGSOC.

Declarations

Ethics approval and consent to participate

Ascites fluid was collected from HGSOC patients who presented for paracentesis at the Royal Hospital for Women, Sydney, between February and December 2022. Samples were obtained with South Eastern Sydney Local Health District Human Research Ethics Committee (SESLHD HREC) approval (reference number 19/001) and informed patient consent. For PA-1 xenograft models, all *in vivo* procedures were approved by the internal ethics and the local government

committees. The animals were handled according to the institutional governmental and European Union guidelines (Austrian Animal Protection Laws and ETS-123, respectively). For PDX models, HGSOC samples were obtained with informed consent from participants who were enrolled in either the Australian Ovarian Cancer Study (AOCS) or the WEHI Stafford Fox Rare Cancer Program (SFRCP). Ethics approval for AOCS was obtained from the Peter MacCallum Cancer Centre Human Research Ethics Committee (HREC) (Melbourne, VIC, Australia) and WEHI SFRCP was approved by Melbourne Health HREC (HREC/15/MH/396), with additional approval from the WEHI HREC (WEHI 10/05 and G16/02).

Consent for publication

All patients have given their informed and written consent to participate in this study, which includes permission to publish any findings. All data have been deidentified to ensure anonymity.

Author contributions

Dongli Liu: Conceptualisation; Data curation; Formal analysis; Investigation; Methodology; Project administration; Software; Visualisation; Writing – original draft.

Cassandra J. Vandenberg: Conceptualisation; Data curation; Formal analysis; Investigation; Methodology; Project administration; Visualisation; Writing – original draft.

Patrizia Sini: Conceptualisation; Funding acquisition; Project administration; Resources; Writing – review & editing.

Lorenz Waldmeier: Conceptualisation; Data curation; Formal analysis; Methodology; Resources; Writing – review & editing.

Rosa Baumgartinger: Data curation; Formal analysis; Methodology; Resources; Writing – review & editing.

Laura Pisarsky: Data curation; Formal analysis; Methodology; Resources; Writing – review & editing.

Georg Petroczi: Data curation; Methodology; Resources.

Gayanie Ratnayake: Data curation; Methodology.

Clare L. Scott: Conceptualisation; Formal analysis; Funding acquisition; Project administration; Supervision; Writing – review & editing.

Caroline E. Ford: Conceptualisation; Formal analysis; Funding acquisition; Project administration; Supervision; Writing – review & editing.

Acknowledgements

We are grateful to the patients who donated biospecimens for this research. We acknowledge Silvia Stoev, Kathy Barber, Chloe Neagle, Stephanie Bound, Dan Fayle and WEHI Bioservices for their excellent technical assistance. We thank the teams at the Histopathology lab at the Garvan Institute of Medical Research, and the WEHI Advanced Histotechnology Facility for providing high-quality services. We thank Mark Radke and Elizabeth Swisher (University of Washington) for the BROCA analysis of PDX models not previously published (#22, #419, #448). We acknowledge Ratana Lim, Briony Milesi, Amanda Lobley, Adriana Acciarino and the contribution of all scientific and clinical staff who have been involved in the WEHI-SFRCP and the patients who have participated in this programme. This work was made possible through the Australian Cancer Research Foundation, the Victorian State Government Operational Infrastructure Support and the Australian Government NHMRC IRIISS.

Funding

The authors disclosed receipt of the following financial support for the research, authorship and/or publication of this article: This work was supported by funding from Boehringer Ingelheim and grants from the Stafford Fox Medical Research Foundation and the National Health and Medical Research Council (NHMRC Australia; Investigator grant 2009783 (CLS)).

Competing interests

C.L.S. and C.J.V. report research support (paid to institution) from AstraZeneca Pty Ltd, Eisai Inc and IDEAYA Biosciences outside the submitted work. C.L.S. reports unpaid advisory boards: AstraZeneca Pty Ltd, Clovis Oncology, Roche, Eisai, Sierra Oncology, Takeda, MSD. L.W. is an employee of NBE-Therapeutics AG.

Availability of data and materials

The author confirms that all data generated or analysed during this study are included in this published article.

ORCID iDs

Dongli Liu https://orcid.org/0000-0002-1755-8516

Laura Pisarsky https://orcid.org/0000-0002-5585-9221

Georg Petroczi https://orcid.org/0000-0003-3069-6013

Supplemental material

Supplemental material for this article is available online.

References

1. Howlader N, Noone A, Krapcho M, et al. SEER cancer statistics review, 1975–2018 (based on November 2020 SEER data submission), https://seer.cancer.gov/csr/1975_2018/ (accessed 1 October 2023).
2. Hoppenot C, Eckert MA, Tienda SM, et al. Who are the long-term survivors of high grade serous ovarian cancer? *Gynecol Oncol* 2018; 148(1): 204–212.
3. Cancer Genome Atlas Research Network. Integrated genomic analyses of ovarian carcinoma. *Nature* 2011; 474(7353): 609–615.
4. Ramus SJ and Gayther SA. The contribution of BRCA1 and BRCA2 to ovarian cancer. *Mol Oncol* 2009; 3(2): 138–150.
5. Pothuri B, O'Cearbhaill R, Eskander R, et al. Frontline PARP inhibitor maintenance therapy in ovarian cancer: a Society of Gynecologic Oncology practice statement. *Gynecol Oncol* 2020; 159(1): 8–12.
6. Tewari KS, Burger RA, Enserro D, et al. Final overall survival of a randomized trial of bevacizumab for primary treatment of ovarian cancer. *J Clin Oncol* 2019; 37(26): 2317.
7. Perren TJ, Swart AM, Pfisterer J, et al. A phase 3 trial of bevacizumab in ovarian cancer. *N Engl J Med* 2011; 365(26): 2484–2496.
8. Oza AM, Cook AD, Pfisterer J, et al. Standard chemotherapy with or without bevacizumab for women with newly diagnosed ovarian cancer (ICON7): overall survival results of a phase 3 randomised trial. *Lancet Oncol* 2015; 16(8): 928–936.
9. Aghajanian C, Blank SV, Goff BA, et al. OCEANS: a randomized, double-blind, placebo-controlled phase III trial of chemotherapy with or without bevacizumab in patients with platinum-sensitive recurrent epithelial ovarian, primary peritoneal, or fallopian tube cancer. *J Clin Oncol* 2012; 30(17): 2039.
10. Coleman RL, Brady MF, Herzog TJ, et al. Bevacizumab and paclitaxel–carboplatin chemotherapy and secondary cytoreduction in recurrent, platinum-sensitive ovarian cancer (NRG Oncology/Gynecologic Oncology Group study GOG-0213): a multicentre, open-label, randomised, phase 3 trial. *Lancet Oncol* 2017; 18(6): 779–791.
11. Bamias A, Gibbs E, Lee CK, et al. Bevacizumab with or after chemotherapy for platinum-resistant recurrent ovarian cancer: exploratory analyses of the AURELIA trial. *Ann Oncol* 2017; 28(8): 1842–1848.
12. Pujade-Lauraine E, Hilpert F, Weber B, et al. Bevacizumab combined with chemotherapy for platinum-resistant recurrent ovarian cancer: the AURELIA open-label randomized phase III trial. *Obstet Gynecol Surv* 2014; 69(7): 402–404.
13. Pujade-Lauraine E, Fujiwara K, Ledermann JA, et al. Avelumab alone or in combination with chemotherapy versus chemotherapy alone in platinum-resistant or platinum-refractory ovarian cancer (JAVELIN Ovarian 200): an open-label, three-arm, randomised, phase 3 study. *Lancet Oncol* 2021; 22(7): 1034–1046.
14. pharma& p. GmbH., pharma& Updates on the Phase 3 ATHENA-COMBO Trial Evaluating rucaparib (Rubraca®) in Combination with nivolumab in First-line Maintenance Treatment in Women with Advanced Ovarian Cancer 2024. https://www.pharmaand.com/wp-content/uploads/2024/05/Rubraca-ATHENA-COMBO-Topline-Data-News-Release-FINAL-.pdf (accessed 8 November 2025).
15. Harter P, Trillsch F, Okamoto A, et al. Durvalumab with paclitaxel/carboplatin (PC) and bevacizumab (bev), followed by maintenance durvalumab, bev, and olaparib in patients (pts) with newly diagnosed advanced ovarian cancer (AOC) without a tumor BRCA1/2 mutation (non-tBRCAm): results from the randomized, placebo (pbo)-controlled phase III DUO-O trial. *J Clin Oncol* 2023; 41(17_suppl): LBA5506.
16. Menck K, Heinrichs S, Baden C, et al. The WNT/ROR pathway in cancer: from signaling to therapeutic intervention. *Cells* 2021; 10(1): 142.
17. Balakrishnan A, Goodpaster T, Randolph-Habecker J, et al. Analysis of ROR1 protein expression in human cancer and normal tissues. *Clin Cancer Res* 2017; 23(12): 3061–3071.
18. Zhang S, Chen L, Wang-Rodriguez J, et al. The onco-embryonic antigen ROR1 is expressed by a variety of human cancers. *Am J Pathol* 2012; 181(6): 1903–1910.

19. Zhang H, Qiu J, Ye C, et al. ROR1 expression correlated with poor clinical outcome in human ovarian cancer. *Sci Rep* 2014; 4(1): 5811.
20. Zhang S, Cui B, Lai H, et al. Ovarian cancer stem cells express ROR1, which can be targeted for anti-cancer-stem-cell therapy. *Proc Natl Acad Sci U S A* 2014; 111(48): 17266–17271.
21. Henry C, Emmanuel C, Lambie N, et al. Distinct patterns of stromal and tumor expression of ROR1 and ROR2 in histological subtypes of epithelial ovarian cancer. *Transl Oncol* 2017; 10(3): 346–356.
22. Kipps TJ. ROR1: an orphan becomes apparent. *Blood* 2022; 140(14): 1583–1591.
23. Quezada MJ and Lopez-Bergami P. The signaling pathways activated by ROR1 in cancer. *Cell Signal* 2023; 104: 110588.
24. Zhao Y, Zhang D, Guo Y, et al. Tyrosine kinase ROR1 as a target for anti-cancer therapies. *Front Oncol* 2021; 11: 680834.
25. Henry C, Llamosas E, Knipprath-Meszaros A, et al. Targeting the ROR1 and ROR2 receptors in epithelial ovarian cancer inhibits cell migration and invasion. *Oncotarget* 2015; 6(37): 40310–40326.
26. Henry C, Hacker N and Ford C. Silencing ROR1 and ROR2 inhibits invasion and adhesion in an organotypic model of ovarian cancer metastasis. *Oncotarget* 2017; 8(68): 112727–112738.
27. Choi MY, Widhopf GF, Ghia EM, et al. Phase I trial: cirmtuzumab inhibits ROR1 signaling and stemness signatures in patients with chronic lymphocytic leukemia. *Cell Stem Cell* 2018; 22(6): 951–959.e3.
28. Lee HJ, Choi MY, Siddiqi T, et al. Phase 1/2 study of cirmtuzumab and ibrutinib in mantle cell lymphoma (MCL) or chronic lymphocytic leukemia (CLL). *J Clin Oncol* 2021; 39: 7556.
29. Shatsky RA, Schwab RB, Helsten TL, et al. Abstract P3-10-18: Phase 1b trial of cirmtuzumab and paclitaxel for locally advanced, unresectable and metastatic breast cancer. *Cancer Res* 2020; 80(4_Suppl.): p. P3-10-18-P3-10-18.
30. Yu J, Chen L, Cui B, et al. Cirmtuzumab inhibits Wnt5a-induced Rac1 activation in chronic lymphocytic leukemia treated with ibrutinib. *Leukemia* 2017; 31(6): 1333–1339.
31. Yin Z, Gao M, Chu S, et al. Antitumor activity of a newly developed monoclonal antibody against ROR1 in ovarian cancer cells. *Oncotarget* 2017; 8(55): 94210.
32. Yin Z, Mao Y, Zhang N, et al. A fully chimeric IgG antibody for ROR1 suppresses ovarian cancer growth in vitro and in vivo. *Biomed Pharmacother* 2019; 119: 109420.
33. Parslow AC, Parakh S, Lee F-T, et al. Antibody–drug conjugates for cancer therapy. *Biomedicines* 2016; 4(3): 14.
34. Ponte JF, Ab O, Lanieri L, et al. Mirvetuximab soravtansine (IMGN853), a folate receptor alpha-targeting antibody-drug conjugate, potentiates the activity of standard of care therapeutics in ovarian cancer models. *Neoplasia* 2016; 18(12): 775–784.
35. Vaisitti T, Arruga F, Vitale N, et al. ROR1 targeting with the antibody-drug conjugate VLS-101 is effective in Richter syndrome patient-derived xenograft mouse models. *Blood* 2021; 137(24): 3365–3377.
36. Jiang VC, Liu Y, Jordan A, et al. The antibody drug conjugate VLS-101 targeting ROR1 is effective in CAR T-resistant mantle cell lymphoma. *J Hematol Oncol* 2021; 14(1): 132.
37. Hu EY, Do P, Goswami S, et al. The ROR1 antibody-drug conjugate huXBR1-402-G5-PNU effectively targets ROR1+ leukemia. *Blood Adv* 2021; 5(16): 3152–3162.
38. Percie du Sert N, Hurst V, Ahluwalia A, et al. The ARRIVE guidelines 2.0: updated guidelines for reporting animal research. *J Cereb Blood Flow Metab* 2020; 40(9): 1769–1777.
39. Beerli RR, Hell T, Merkel AS, et al. Sortase enzyme-mediated generation of site-specifically conjugated antibody drug conjugates with high in vitro and in vivo potency. *PLoS One* 2015; 10(7): e0131177.
40. Shepherd TG, Thériault BL, Campbell EJ, et al. Primary culture of ovarian surface epithelial cells and ascites-derived ovarian cancer cells from patients. *Nat Protoc* 2006; 1(6): 2643–2649.
41. Liu D, Gunther K, Enriquez LA, et al. ROR1 is upregulated in endometrial cancer and represents a novel therapeutic target. *Sci Rep* 2020; 10(1): 13906.
42. Ianevski A, Giri AK and Aittokallio T. SynergyFinder 2.0: visual analytics of multi-drug combination synergies. *Nucleic Acids Res* 2020; 48(W1): W488–W493.
43. Kondrashova O, Topp M, Nesic K, et al. Methylation of all *BRCA1* copies predicts response to the PARP inhibitor rucaparib in ovarian carcinoma. *Nat Commun* 2018; 9: 3970.
44. Ho GY, Vandenberg CJ, Lim R, et al. The microtubule inhibitor eribulin demonstrates

efficacy in platinum-resistant and refractory high-grade serous ovarian cancer patient-derived xenograft models. *Ther Adv Med Oncol* 2023; 15: 17588359231208674.

45. Nesic K, Krais JJ, Vandenberg CJ, et al. BRCA1 secondary splice-site mutations drive exon-skipping and PARP inhibitor resistance. medRxiv, 2023.
46. Sharma SK, Chow A, Monette S, et al. Fc-mediated anomalous biodistribution of therapeutic antibodies in immunodeficient mouse models. *Cancer Res* 2018; 78(7): 1820–1832.
47. Liu K, Li M, Li Y, et al. A review of the clinical efficacy of FDA-approved antibody–drug conjugates in human cancers. *Mol Cancer* 2024; 23(1): 62.
48. Hojjat-Farsangi M, Khan AS, Daneshmanesh AH, et al. The tyrosine kinase receptor ROR1 is constitutively phosphorylated in chronic lymphocytic leukemia (CLL) cells. *PLoS One* 2013; 8(10): e78339.
49. Kaucká M, Krejčí P, Plevová K, et al. Post-translational modifications regulate signalling by Ror1. *Acta Physiol* 2011; 203(3): 351–362.
50. Pujade-Lauraine E, Wagner U, Aavall-Lundqvist E, et al. Pegylated liposomal doxorubicin and carboplatin compared with paclitaxel and carboplatin for patients with platinum-sensitive ovarian cancer in late relapse. *J Clin Oncol* 2010; 28(20): 3323–3329.